Petrology, Vol. 9, No. 6, 2001, pp. 516–533. Translated from Petrologiya, Vol. 9, No. 6, 2001, pp. 593–611.

Zonal Metamorphism and Petrology of Metapelites in the Tim–Yastrebovskaya Structure, Voronezh Crystalline Massif

K. A. Savko and T. N. Polyakova

Voronezh State University, Universitetskaya pl. 1, Voronezh, 394693 Russia
e-mail: gfkig304@main.vsu.ru

Received February 15, 2001

Abstract—Our detailed petrographic study of the Early Proterozoic metapelites of the Tim–Yastrebovskaya structure resulted in distinguishing the following four metamorphic zones: garnet–chlorite, staurolite–andalusite, staurolite–sillimanite, and sillimanite–muscovite. The zoning mapped in the area is noted for the fact that its Mn-rich metapelites contain the assemblage of Fe–Mn garnet with andalusite in place of staurolite. Based on its morphology, composition, and zoning, the garnet of the rocks can be subdivided into two types: early kinematic with prograde zoning and late kinematic with retrograde zoning or unzoned. The results of microthermometry and mineralogical thermobarometry led us to conclude that the metapelites of the Tim–Yastrebovskaya structure were affected by two metamorphic events. During the early episode, which was related to folding at 2250 Ma, the metasediments were regionally metamorphosed to the garnet–chlorite grade (zone). The intrusion of large granodiorite bodies at 2086 Ma induced the second metamorphic episode, during which the metapelites were metamorphosed at 520–620°C and 3–4 kbar.

INTRODUCTION

The advances achieved over the past two decades in precise techniques for the assaying the physicochemical conditions of lithospheric mineralizing processes made it possible to model geodynamic environments in correlations with various types of physicochemical metamorphic conditions (Glebovistkii, 1996; Reverdatto *et al.*, 1995; De Yoreo *et al.*, 1991; England and Thompson, 1984).

Metamorphic zoning is commonly interpreted as reflecting either the spatial distribution of local heat fluxes (thermal dome model) or the regional *P–T* gradients during the subsidence of crustal blocks (gradient model), with the temperature of the latter model depending exclusively on the burial depth of the rocks (Dobretsov *et al.*, 1970; Korikovskii, 1995). However, metamorphic zoning can also be induced by intruded magmatic bodies (contact regional metamorphism).

Detailed data obtained on the metapelites of the Tim–Yastrebovskaya structure demonstrate that its metamorphic zoning was caused by the effect of intrusions of various compositions. Another distinctive feature of the rocks is the rarity of staurolite in mineral assemblages whose temperature and pressure correspond to the conditions of the staurolite and staurolite–sillimanite grades. Because of this, the possibility of mapping this metamorphic zoning based on such an important index mineral as staurolite was limited, and information on the evolution of the thermodynamic metamorphic parameters could be obtained with the utilization of data of microstructural analysis and the chemistry of minerals. The minerals of the Tim–Yastrebovskaya metapelites most suitable for these purposes are garnet and micas.

This study was centered on the analysis of mineral assemblages from the zonal metamorphic aureole of the Tim–Yastrebovskaya structure. Much attention was focused on studying the morphology, chemistry, and zoning of garnet with the aim of reproducing the evolution of the physicochemical metamorphic parameters.

GEOLOGY

The Voronezh crystalline massif is a large, shallowly buried uplift of the East European Platform basement. The massif is composed of three major types of structures: Early Archean gneiss–migmatite and granulite blocks, Late Archean granite–greenstone belts, and Early Proterozoic mobile belts, which are restricted to regional deep faults between Early Archean blocks (Fig. 1).

The Tim–Yastrebovskaya structure in the Alekseevsko–Voronezh tectono–stratigraphic terrane is one of the largest Early Proterozoic strictures of the Voronezh crystalline massif. It extends for 130 km from northwest to southeast, has a width of 10–30 km, and, according to geophysical evidence, is characterized by a depth of 5–8 km. The thickness of the Phanerozoic sedimentary cover that overlies the Precambrian rocks within the structure is 57–214 m, and, hence, all conclusions cited in this paper were arrived at based on a detailed study of the drilling core.

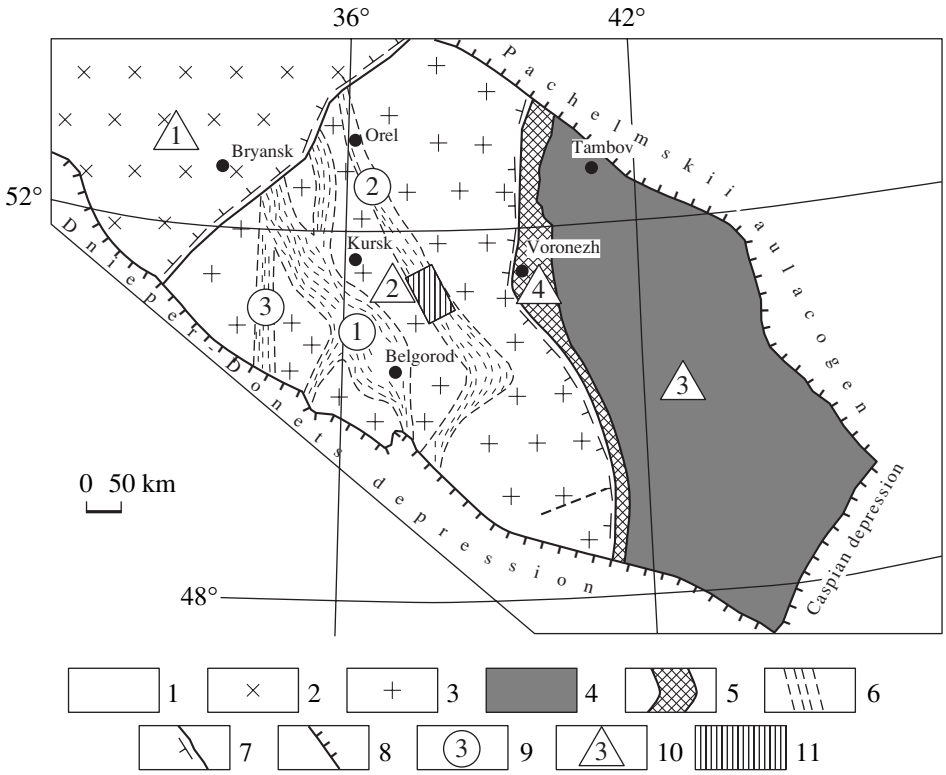

Fig. 1. Schematic structural–geological map of the Voronezh crystalline massif (modified after Chernyshov *et al.*, 1997).
(1–6) Tectono–stratigraphic complexes: (1) Riphean and Phanerozoic platform complexes, (2–6) pre-Riphean complexes (2, 3) of the Bryansk and Kursk megablocks of the Early Archean consolidation, (4) Vorontsovskii pericraton trough, (5) Livny–Bogucharskaya suture, (6) second-order Riphean structures); (7–8) geologic boundaries: (7) between megablocks, (8) of the Voronezh crystalline massif; (9) second-order riftogenic structures (circled numbers: 1—Belgorod–Mikhailovskaya, 2—Orel–Timskaya, 3—Krupetsko–Krivoi Rog); (10) first-order structures (numbers in triangles: 1—Bryansk megablock, 2—Kursk megablock, 3—Voronezh megablock, (4)—Livny–Bogucharskaya suture): (11) the Tim–Yastrebovskaya structure (study area).

The basement on which the Tim–Yastrebovskaya structure was formed in the Early Proterozoic consisted of thick masses of high-grade metamorphosed sedimentary and volcano-sedimentary rocks of the Oboyanskaya and Mikhailovskaya groups of Archean age.

The Oboyanskaya Group is dominated by granite-gneisses, migmatites, and biotite–plagioclase, garnet–biotite–plagioclase, amphibole–plagioclase, and quartz–feldspar gneisses. The granite-gneiss fields include relatively thin bodies of granulites, eulysites, and amphibolites.

The Mikhailovskaya Group is composed of ortho-amphibolites and orthoschists of mafic and ultramafic composition, pyroxenite and peridotite komatiites, rhyolites, rhyodacites, dacites, quartz–biotite, quartz–two mica, and quartz–chlorite schists, and more rare sandstones, quartzites and occasional thin bodies of jaspilites. The rocks are often migmatized.

The Tim–Yastrebovskaya structure includes the Early Proterozoic Kurskaya and Oskol'skaya groups, which are extensively folded and metamorphosed. All of the stratified rocks are characterized by a systematic transitions from terrigenous–sedimentary to terrigenous–carbonate and terrigenous–volcanic rocks with increasing concentrations of carbonaceous matter and volcanic material.

The rocks of the Kurskaya Group occur in the southwestern flank of the Tim–Yastrebovskaya structure (Fig. 2) and are dominated by quartz–mica schists and jaspilites.

The Oskol'skaya Group is characterized by cyclical intercalations of conglomerates, gritstones, and metasandstones, which upward grade into carbonate–micaceous schists with beds of amphibolites and metamorphosed limestones and dolomites and abundant rocks with carbonaceous matter and volcanics. The group consists of two conformable formations: the lower Rogovskaya terrigenous–carbonate and the upper Timskaya terrigenous–volcanic formations.

The rocks of the Rogovskaya Formation are exposed in the southwestern flank and the southern structural closure of the Tim–Yastrebovskaya structure (Fig. 2). These are quartz–biotite, quartz–muscovite, quartz–garnet–biotite, and quartz–biotite–staurolite schists with thin beds of carbonate rocks, metasandstones, and amphibolites.

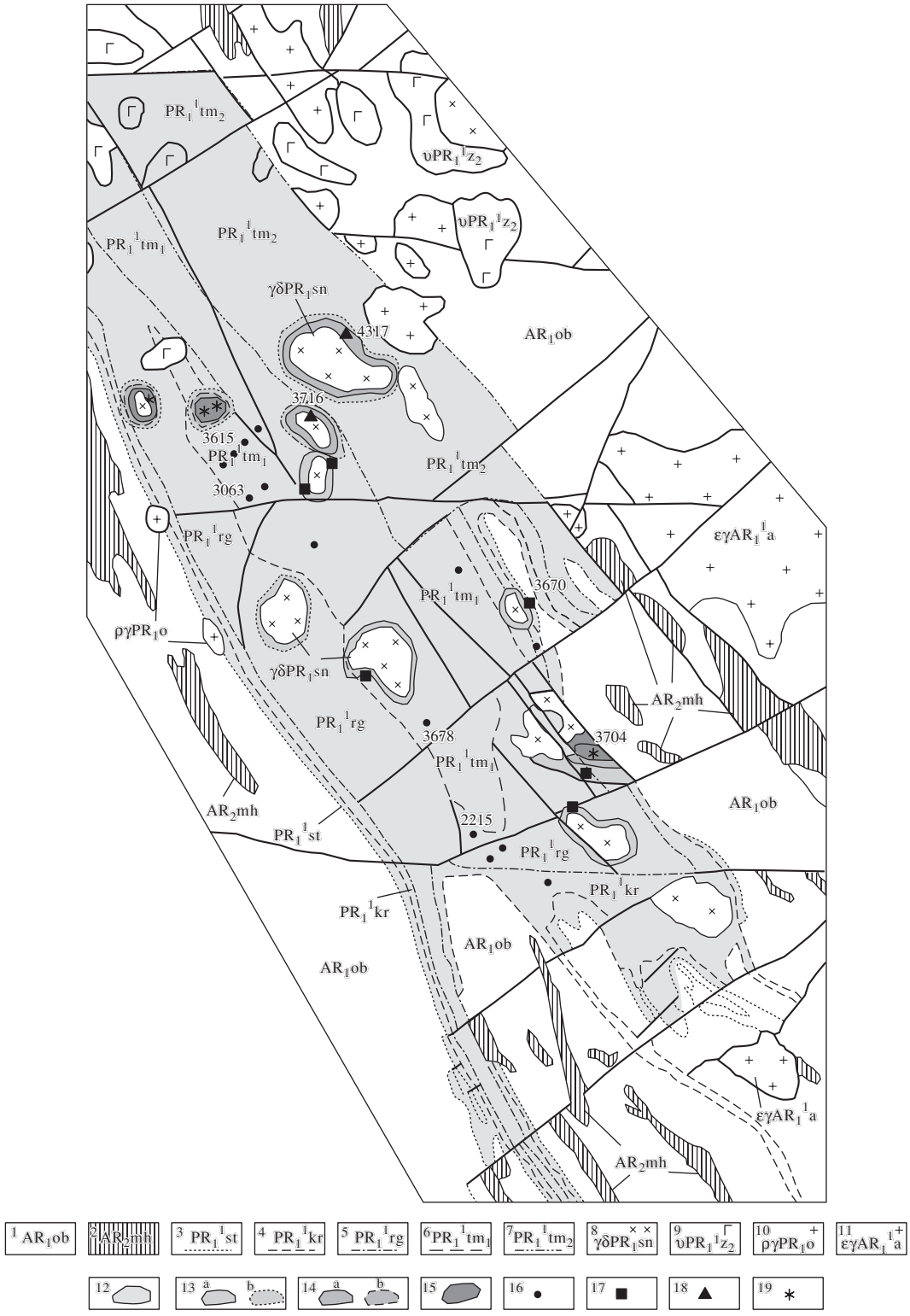

Fig. 2. Schematic geological map of the Tim–Yastrebovskaya structure and metamorphic zoning in its metapelites (based on materials borrowed from Voronezhgeologiya State Geological Enterprise).

(1) Oboyanskaya Group; (2) Mikhailovskaya Group. Geologic boundaries: (3–4) Kursk Group, (3) Stoilenskaya Formation and (4) Korobkovskaya Formation); (5–7) Oskol Group (5) Rogovskaya Formation, (6) Timskaya Formation, lower subformation, (7) Timskaya Formation, upper subformation); (8–11) intrusive complexes (8) Stoilo–Nikolaevskii, (9) Zolotukhinskii, (10) Oskoletskii, (11) Atamanskii; (12–15) metamorphic zones (12) garnet–chlorite, (13) staurolite–andalusite, (14) staurolite–sillimanite, (a) observed, (b) inferred, (15) sillimanite–muscovite); (16–19) sampling sites for rocks with index minerals (16) garnet, (17) garnet + andalusite, staurolite, (18) staurolite + sillimanite, (19) muscovite + sillimanite). Numbers of holes are given for analyzed samples.

The composition of the Timskaya Formation, which makes up the central part of the structure, is determined by widespread carbonaceous sulfidized schists with subordinate amounts of beds and strata of metasandstones, quartzites, calc-silicate rocks, marbles, and volcanic rocks.

The rocks of the Oskol'skaya Group were dated by U–Pb techniques on zircon from acid volcanics and syngenetic metapelites (Artemenko *et al.*, 1992). The Timskaya metadacites were dated in the northern portion of the structure (Hole 4067, depth interval 479.0–493.5 m). Dikes of quartz metaporhyries and two-mica granite porphyries were studied in the drill core from the eastern part of the Tim–Yastrebovskaya structure (Hole 4310, depth interval 457.4–462.0 m, and Hole 4043, depth interval 337.0–352.0 m, respectively). The U–Pb isochron plots with concordia date the volcanic event at 2167 ± 288 Ma for the metadacite and 2254 Ma for the quartz metaporphyries. The relatively high errors of the former isochron date is explained by the small spread of the U–Pb isotopic ratios for distinct zircon fractions from this sample. Hence, the isotopic age of the sedimentary–volcanic rocks of the Oskol'skaya Group is 2250 Ma.

The igneous rocks of the structure belong to the premetamorphic Atamanskii Complex of moderately alkaline granites (plagioclase–microcline biotite granites) and the Oskoletskii Complex of migmatitic plagiogranites (plagiogranite, granodiorite, adamellite, and granite) and to the postmetamorphic Stoilo–Nikolaevskii dike complex of the gabbro–diorite–granodiorite association (granodiorite, gabbro, diorite, quartz diorite) and the Zolotukhinskii peridotite–gabbronorite complex (gabbronorite, gabbro, diorite, peridotite, and serpentinite) (Fig. 2).

The intrusive rocks of the Stoilo–Nikolaevskii Complex were isotopically dated on biotite–hornblende mesodiorite (Hole 4071, depth interval 480.5–488.3 m) and granodiorite (Hole 4074, depth interval 261.0–262.9 m) (Artemenko *et al.*, 1992). Because the U–Pb isotopic ratios of zircon from these samples were characterized by very insignificant distinctions, a single concordia plot was calculated for both of them, which determined an isotopic age of 2086 ± 5 Ma.

PETROGRAPHY

Metapelites are widespread in the Tim–Yastrebovskaya structure. These are light or dark gray to black fine- and medium-grained quartz–biotite, quartz–muscovite, garnet–quartz–biotite, staurolite–quartz–biotite, andalusite, cordierite, and carbonaceous schists. In accordance with their chemistry, they can be classed into high- and low-Mn groups. Some varieties of the carbonaceous and micaceous–carbonaceous schists contain up to 9 wt % MnO (Table 1).

A detailed petrographic study of the metapelites let us recognize the following four metamorphic zone: garnet–chlorite, staurolite–andalusite, staurolite–sillimanite, and sillimanite–muscovite. The zones are separated with isograde, which reflect prograde metamorphic reactions that describe changes in the critical mineral assemblages. The garnet–chlorite zone covers the largest area within the structure, and the staurolite–andalusite, staurolite–sillimanite, and sillimanite–muscovite zones occur locally and are restricted to contact aureoles around intrusions (Fig. 2). The boundaries between metamorphic zones are drawn based on rocks recovered by holes and containing index minerals. The possibility of mapping metamorphic zones in narrow contact aureoles on the basis of core materials alone is limited, and, thus, some boundaries in our map are shown schematically.

The most ubiquitous mineral assemblages are *Qtz* + *Pl* + *Bt* + *Grt* + *Chl* + *Gr* for the garnet–chlorite zone, *Qtz* + *Pl* + *Bt* + *Ms* + *And* + *Grt* + *Chl* ± *St* for the staurolite–andalusite zone, *Qtz* + *Pl* + *Bt* + *St* + *Sil* + *Grt* + *And* for the staurolite–sillimanite zone, and *Qtz* + *Pl* + *Sil* + *Ms* + *Bt* for the sillimanite–muscovite zone.

The characteristic mineral assemblages of each of the zones are listed in Table 2.

The accessory minerals are apatite, sphene, tourmaline, pyrite, pyrrhotite, chalcopyrite, and magnetite.

METHODS

All of our samples are fragments of the core, which was thoroughly described during the fieldworks. The samples were examined under an optical microscope, and the minerals of assemblages with the least number of freedom degrees were then analyzed on a laser microprobe. Spot analyses of minerals were conducted on a Camebax SX-50 microprobe at the Moscow State University at an accelerating potential of 15 kV, beam current of 1–2 nA, and beam diameter of 1–2 μm. The accuracy of the analyses was systematically controlled by analyzing natural and synthetic standards. The cation proportions were normalized to the following numbers of oxygen atoms: 12 for garnet, 46 for staurolite, 11 for muscovite and biotite, 8 for plagioclase, and 14 for chlorite. The *P–T* metamorphic conditions were calculated by the PTF (Fonarev *et al.*, 1991) and GEOPATH (Gerya and Perchuk, 1992) computer programs.

Back-scattered electron images of thin sections were obtained on a CamScan electron microscope equipped with a Link EDS device at Moscow State University.

MINERAL CHEMISTRY

The garnet-bearing metapelites from the Tim–Yastrebovskaya structure contain quartz, plagioclase, biotite, muscovite, chlorite, staurolite, sillimanite, andalusite, and cordierite.

Quartz and plagioclase account for 20–30 modal % in most of our samples. The plagioclase is relatively

Table 1. Chemical composition (wt %) of metapelites of the Tim–Yastrebovskaya structure

Component	1	2	3	4	5	6	7	8	9	10	11	12
SiO_2	53.18	57.22	54.80	56.18	39.68	41.58	57.17	57.80	49.26	55.46	50.20	41.88
TiO_2	0.92	0.97	0.74	0.82	4.50	0.43	0.75	0.83	1.30	–	0.20	0.11
Al_2O_3	15.88	15.80	18.50	20.41	7.92	3.08	15.56	7.60	13.64	12.72	14.38	3.94
Fe_2O_3	1.33	1.03	1.56	1.00		0.76	1.05	1.75	1.20	2.39	6.20	7.91
FeO	8.22	6.16	7.67	6.74	14.05	17.31	1.23	6.33	7.53	7.38	7.50	8.62
MnO	0.13	0.15	0.07	0.04	0.17	0.44	8.86	1.80	0.24	0.08	0.43	0.07
MgO	4.23	4.09	4.10	1.99	7.73	3.31	2.48	6.00	6.92	10.11	3.43	24.99
CaO	4.17	3.26	2.60	0.74	9.57	7.71	1.55	2.21	9.11	4.55	0.89	0.56
Na_2O	1.68	1.55	3.64	0.25	0.10	0.31	0.13	0.24	1.00	1.60	0.28	0.24
K_2O	2.95	3.16	3.32	7.98	1.90	1.08	2.10	1.63	4.20	2.02	1.36	0.85
P_2O_5	0.25	0.29	0.19	0.12	1.01	2.95	0.24	0.22	0.27	0.03	0.03	0.01
SO_3	–	–	–	–	3.14	9.51	0.93	3.40	1.37	0.83	5.34	5.83
CO_2	–	–	–	–	–	12.00	5.50	6.20	–	–	–	–
Total	99.90	99.86	99.19	99.27	98.94	100.26	99.47	99.49	100.30	99.17	99.24	99.01

Note: (1) Biotite–quartz schist (Hole 3630/285.6); (2) sericite–quartz schist (Hole 3629/259.2); (3) cordierite–quartz-biotite schist (Hole 3129/333.0); (4) muscovite schist (Hole 3611/251.1); (5) quartz-plagioclase–biotite schist (Hole 3123/235.8); (6) carbonaceous quartz schist (Hole 3063/618.0); (7) carbonaceous quartz schist (Hole 3063/250.0); (8) carbonaceous schist (Hole 3053/216.0); (9) quartz–biotite schist (Hole 3654/391.0); (10) quartz–biotite schist (Hole 992/176.0); (11) carbonaceous quartz–mica schist (Hole 993/162.0); (12) quartz–biotite schist (Hole 999/164.0). Analyses were conducted at the chemical laboratory of the Voronezhgeologia State Geological Enterprise.

Table 2. Mineral assemblages of metapelites of the Tim–Yastrebovskaya structure

Sample	Rock	Metamorphic zone	Mineral assemblage
3063/1a	Carbonaceous schist	Garnet–chlorite	*Qtz* + $Pl_{Na>}$ + *Kfs* + *Bt* + *Ms* + *Grt* + *Cal* + *Spn* + *Gr*
3615/1	Quartz–muscovite schist	"	*Qtz* + *Pl* + *Ms* + *Grt* + *Gr*
2215/9	Garnet schist	"	*Qtz* + *Pl* + *Grt* + *Chl* + *Gr*
2207/2a	Quartz–biotite schist	"	*Qtz* + *Pl* + *Bt* + *Grt* + *Chl* + *Gr*
3678/256.0	Quartz–muscovite schist	"	*Qtz* + *Pl* + *Bt* + *Ms* + *Grt* + *Gr*
3129/317.3	Cordierite schist	Staurolite–andalusite	*Qtz* + *Pl* + *Crd* + *Gr*
3129/3	Andalusite schist	"	*Qtz* + *Pl* + *Bt* + *And* + *Gr*
3706/331.0	Quartz–biotite schist	"	*Qtz* + *Pl* + *Bt* + *Chl* + *Grt* + *St* + *Ms*
3670/1	Quartz–biotite schist	"	*Qtz* + *Pl* + *Bt* + *Ms* + *Grt* + *St*
3702/9	Quartz–biotite schist	"	*Qtz* + *Pl* + *Bt* + *Grt*
4317/397.0	Quartz–biotite schist	Staurolite–sillimanite	*Qtz* + *Pl* + *Grt* + *Crd*
4317/370.1	Quartz–biotite schist	"	*Qtz* + *Pl* + *Bt* + *Grt*
4317/604.5	Quartz–biotite schist	"	*Qtz* + *Bt* + *Ms* + *And*
3716/1b	Quartz–biotite schist	"	*Qtz* + *Pl* + *Bt* + *Ms* + *Grt* + *St* + *And* + *Sil*
3704/17	Quartz–muscovite schist	Sillimanite–muscovite	*Qtz* + *Pl* + *Bt* + *Ms* + *Sil* + *Gr*
3704/20	Quartz–biotite schist	"	*Bt* + *Grt* + (*St*)
3634/8	Crystalline schist	"	*Qtz* + *Pl* + *Ms* + *Bt* + *Sil*

rarely twinned. The quartz–biotite schists of the garnet–chlorite zone bear plagioclase from $An_{40–52}$ to An_{62} (Table 3). The carbonaceous schists of the garnet–chlorite zone contain albite-oligoclase with an insignificant admixture of anorthite, An_{11} (Table 3).

The *biotite* is light to dark brown or has a brownish or greenish color and volumetrically dominates over other micas in the rocks of any metamorphic zone. It occurs as very small flakes in the garnet–chlorite zone and as larger laths (1–2 mm) in the higher temperature

zones. The iron mole fraction of the mineral, $X_{Fe} = Fe^{+2}/(Fe^{+2} + Mg)$ at. %, varies within broad limits, from 33 to 64% (Table 4), due to variations in the chemical composition of the rocks. The TiO_2 concentration in the mineral systematically increases with increasing temperature from 1.02–1.15 wt % in the garnet–chlorite zone to 1.62–2.34 wt % in the staurolite–sillimanite zone (Table 4).

The mica of the carbonaceous sulfide-bearing schists (Sample 3063/1a) approaches phlogopite in composition (X_{Fe} = 3–15%) (Table 4).

Muscovite occurs in the metapelites of the garnet–chlorite zone as small flakes. As the metamorphic grade increases, the size of the flakes also increases, so that the rocks of the staurolite–sillimanite zone contain relatively large (up to 1 mm) platelets. We detected no clearly pronounced tendencies in the variations in the paragonite and phengite concentrations (Table 5).

Staurolite. In spite of the fact that the *P–T* conditions of metapelites near intrusions correspond to the staurolite–andalusite and staurolite–sillimanite subfacies, staurolite itself is very rare in these rocks. This is caused, first of all, by the chemistry of the rocks. As was mentioned above, the Tim–Yastrebovskaya structure contains rocks whose protoliths were Mn-enriched sediments (Table 1). These low-Fe and high-Mn metapelites only very rarely contain staurolite or do not bear it at all, because Fe–Mn garnet is an alternative stable mineral in assemblages with andalusite and biotite (Korikovskii, 1979).

Relatively Fe- and Al-rich rocks with "normal" Mn concentration contain oval or anhedral unzoned staurolite grains. Staurolite of the staurolite–andalusite zone has an average $X_{Fe} \approx 88\%$ and contains minor amounts of ZnO (0.09–0.36 wt %), whose concentration decreases rimward. The iron mole fraction of staurolite in the staurolite–sillimanite zone decreases to 82–84%, and its ZnO concentration notably increases (to 1.55–1.85 wt %) (Table 6). This composition is typical of staurolite in the high-temperature part of the staurolite–sillimanite zone. The high ZnO concentration is caused by a decrease in the staurolite content toward the high-temperature part of the facies, with Fe-rich staurolite being the first to decompose, Zn-enriched varieties surviving to higher temperatures, and the last remaining crystals becoming strongly enriching in Zn. It is the Zn presence in staurolite in the form of a phase-forming component that causes the stability of this mineral near the boundary of the staurolite facies (Korikovskii, 1979). In the sillimanite–muscovite zone, staurolite is preserved only in the form of relict armored inclusions in other minerals (Savko, 1994). One of such grains included in garnet (Sample 3704/20) had X_{Fe} = 88–89% and contained 0.66–0.67 wt % ZnO (Table 6).

The primary *chlorite* of the Tim–Yastrebovskaya metapelites occurs before the staurolite–sillimanite zone. This mineral in assemblage with garnet in the garnet–chlorite zone has X_{Fe} = 50–52% (Table 5).

Table 3. Microprobe analyses of plagioclase from metapelites of the Tim–Yastrebovskaya structure

Component	Garnet–chlorite zone			
	3063/1	3678/256.0		
SiO_2	66.53	53.49	56.44	56.09
Al_2O_3	21.28	30.25	28.19	25.98
FeO	–	–	–	1.96
MgO	–	–	–	1.96
CaO	2.03	11.85	9.94	7.21
Na_2O	9.82	4.08	5.18	5.29
K_2O	0.1	0.09	0.04	1.21
Total	99.7	99.7	99.8	99.7
	8 O			
Si	2.91	2.41	2.53	2.54
Al	1.10	1.61	1.49	1.39
Fe^{+2}	–	–	–	0.07
Mg	–	–	–	0.13
Ca	0.10	0.57	0.48	0.35
Na	0.83	0.36	0.45	0.46
K	0.01	0.01	–	0.07
Ab	0.89	0.38	0.48	0.53
An	0.11	0.62	0.52	0.40
Or	–	–	–	0.07

Andalusite occurs in the staurolite–andalusite and staurolite–sillimanite zones as anhedral or oval grains, often with pronounced cleavage and abundant quartz inclusions. The staurolite–sillimanite zone contains both alumina silicates as equilibrium minerals.

Sillimanite develops in the form of fibrolite, which often growths through biotite crystals.

Cordierite was encountered in hornfels close to the contact with intrusive rocks and typically had sectorial trillings and sixlings.

COMPOSITION AND ZONING OF GARNET

Our detailed studies of thin sections of metapelites from the zonal complex let us confidently distinguish two generations of minerals, which corresponded to two episodes of the metamorphic evolution: early and late kinematic.

Garnet. The garnet of the early-kinematic generation occurs in metapelites of the Tim–Yastrebovskaya structure only within the garnet–chlorite zone. It composes porphyroblasts of equant or irregular shapes with clear pressure shadows (Fig. 3a) and contains abundant oriented inclusions of quartz, plagioclase, and carbonaceous matter, which compose trails and characteristic "petal" patterns (Figs. 3d, 3g). Garnet from the carbon-

Table 4. Microprobe analyses of biotite from metapelites of the Tim–Yastrebovskaya structure

Component	Garnet–chlorite zone					Staurolite–andalusite zone	Staurolite–sillimanite zone				Sillimanite–muscovite zone	
	3678/256.0			3063/1		3670/1	4317/370.1	3716/1			3704/20	
	matrix			matrix		matrix	incl. in *Grt*	matrix			matrix	
	Bt-21	*Bt*-23	*Bt*-26	*Bt*-7	*Bt*-10	*Bt*-13	*Bt*-18	*Bt*-5	*Bt*-6	*Bt*-10	*Bt*-50	*Bt*-51
SiO_2	44.99	38.90	41.03	36.54	40.27	43.35	36.74	35.88	35.63	31.73	31.71	32.21
Al_2O_3	16.85	18.76	21.73	17.53	18.16	26.05	17.94	20.45	19.98	20.87	15.45	16.04
TiO_2	1.13	1.15	1.02	0.75	1.07	1.50	1.69	2.34	2.30	2.00	0.58	0.58
Cr_2O_3	0.08	–	0.38	0.18	0.43	0.19	0.14	0.07	0.20	0.14	–	0.06
FeO	11.69	12.75	12.16	5.95	3.95	11.09	21.73	21.76	22.55	25.98	29.08	27.62
MnO	0.26	0.38	0.21	1.15	0.76	–	–	0.06	0.08	0.14	0.04	–
MgO	12.50	14.38	12.61	18.89	20.10	4.66	10.12	7.15	7.13	8.84	12.67	11.15
CaO	0.46	0.12	0.09	4.92	0.18	0.10	0.15	0.03	0.05	0.06	0.10	0.02
Na_2O	0.28	0.16	0.12	0.04	0.20	0.10	0.26	0.18	0.20	0.17	0.25	0.22
K_2O	8.03	9.57	7.39	8.49	9.66	7.00	8.01	8.52	8.54	5.54	3.77	6.04
ZnO	–	–	–	–	–	0.15	–	0.05	–	–	0.17	–
ClO	0.12	0.15	0.09	–	–	0.05	0.22	–	0.05	–	0.20	0.13
Total	96.35	96.32	96.83	94.48	94.78	94.24	96.96	96.52	96.71	95.44	94.00	94.07
11 O												
Si	3.17	2.82	2.88	2.68	2.85	3.08	2.76	2.70	2.69	2.45	2.54	2.58
Al(IV)	0.83	1.18	1.12	1.33	1.15	0.92	1.23	1.3	1.31	1.55	1.45	1.42
Al(VI)	0.57	0.43	0.68	0.19	0.37	1.27	0.34	0.52	0.47	0.35	–	0.09
Ti	0.06	0.06	0.05	0.04	0.06	0.70	0.10	0.13	0.13	0.12	0.04	0.04
Cr	–	–	0.02	0.01	0.02	0.01	0.01	–	0.01	0.01	–	–
Fe^{+2}	0.69	0.77	0.72	0.36	0.23	0.66	1.36	1.37	1.43	1.68	1.95	1.85
Mn	0.02	0.02	0.01	0.07	0.05	–	–	0.01	0.01	0.01	–	–
Mg	1.31	1.56	1.32	2.06	2.12	0.49	1.13	0.80	0.80	1.02	1.50	1.33
Ca	0.04	0.01	0.01	0.39	0.01	0.01	0.01	–	–	0.01	0.01	–
Na	0.04	0.02	0.02	0.01	0.03	0.01	0.04	0.03	0.03	0.03	0.04	0.03
K	0.72	0.89	0.66	0.79	0.87	0.63	0.77	0.82	0.82	0.55	0.39	0.62
Zn	–	–	–	–	–	0.01	–	–	–	–	0.01	–
Cl	0.01	0.02	0.01	–	–	–	0.03	–	0.01	–	0.03	0.02
$Fe^{+2}/(Fe^{+2} + Mg)$	0.34	0.33	0.35	0.15	0.10	0.57	0.55	0.63	0.64	0.62	0.57	0.58

Table 5. Microprobe analyses of chlorite and muscovite from metapelites of the Tim–Yastrebovskaya structure

Component	Garnet–chlorite zone										Staurolite–andalusite zone	Staurolite–sillimanite zone	
	2215/9				3615/1					3063/1	3670/1	3716/1	
	matrix												
	Chl-2	*Chl*-3	*Chl*-4	*Chl*-5	*Ms*-45	*Ms*-46	*Ms*-47	*Ms*-48	*Ms*-49	*Ms*-9	*Ms*	*Ms*-7	*Ms*-8
SiO_2	26.97	25.86	26.09	26.67	50.23	47.16	46.02	48.86	45.40	47.18	47.03	47.25	47.62
Al_2O_3	24.14	21.88	24.98	25.18	33.64	37.08	37.16	37.34	35.87	32.77	37.05	38.42	37.45
TiO_2	–	0.06	0.05	0.08	0.44	0.52	0.57	0.62	0.71	0.28	0.62	0.33	0.39
Cr_2O_3	0.07	1.45	0.10	0.22	–	0.30	0.13	0.12	0.71	1.01	0.50	0.19	0.03
FeO	27.11	26.17	27.93	26.76	1.51	1.25	1.04	1.16	2.31	0.82	1.07	1.20	1.03
MnO	0.11	0.05	0.09	0.11	0.02	0.05	–	–	–	0.03	–	0.20	–
MgO	15.45	13.14	14.60	14.48	1.75	0.77	0.63	0.65	1.07	2.71	0.62	0.39	0.43
CaO	0.13	0.15	0.13	0.13	–	0.03	–	–	0.06	0.08	0.08	0.06	0.02
Na_2O	0.01	0.05	0.02	0.01	0.43	0.62	0.59	0.64	0.67	0.33	1.04	0.79	0.88
K_2O	0.03	0.02	0.05	0.03	10.0	9.81	10.21	10.15	9.44	10.35	9.11	8.64	9.46
ClO	0.04	–	0.07	0.04	–	–	–	–	–	–	0.04	0.06	0.02
Total	94.05	88.89	94.10	93.71	98.03	97.56	96.35	97.53	96.23	95.55	97.17	97.79	97.33
	14 O				11 O								
Si	2.65	2.70	2.57	2.62	3.23	3.05	3.02	3.04	3.00	3.13	3.05	2.04	3.07
Al(IV)	1.35	1.30	1.43	1.38	0.77	0.95	0.98	0.97	1.00	0.87	2.83	0.97	0.93
Al(VI)	1.44	1.40	1.48	1.53	1.77	1.88	1.89	1.89	1.80	1.70	0.03	1.94	1.92
Ti	0.01	0.12	–	0.02	0.02	0.03	0.03	0.03	0.04	0.01	0.03	0.02	0.02
Fe^{+2}	2.23	2.29	2.30	2.22	0.08	0.07	0.06	0.06	0.13	0.05	0.06	0.06	0.06
Mn	0.01	–	0.01	0.01	–	–	–	–	–	–	–	0.01	–
Mg	2.26	2.05	2.15	2.12	0.17	0.07	0.06	0.06	0.11	0.27	0.06	0.04	0.04
Ca	0.01	0.02	0.01	0.01	–	–	–	–	–	0.01	0.01	–	–
Na	–	0.01	–	–	0.05	0.08	0.08	0.08	0.09	0.04	0.13	0.10	0.11
K	–	–	0.06	–	0.82	0.81	0.86	0.84	0.80	0.88	0.75	0.71	0.78
Cl	0.01	–	0.01	0.01	–	–	–	–	–	–	0.01	0.01	–
$Fe^{+2}/(Fe^{+2} + Mg)$	0.50	0.52	0.50	0.51									
Pg					0.06	0.09	0.09	0.09	0.10	0.04	0.14	0.04	0.04
Phn					0.11	0.08	0.07	0.08	0.13	0.16	0.80	0.11	0.12

Table 6. Microprobe analyses of staurolite from metapelites of the Tim–Yastrebovskaya structure

Component	Staurolite–andalusite zone			Staurolite–sillimanite zone				Sillimanite–muscovite zone		
	3670/1			3716/1				3704/20		
	core	margin	core	core	margin		core	incl. in *Grt*		
	St-15	*St*-16	*St*-17	*St*-1	*St*-2	*St*-3	*St*-4	*St*-40	*St*-48	*St*-49
SiO_2	27.97	26.94	28.42	27.43	27.74	27.97	28.10	27.89	27.76	27.93
Al_2O_3	55.55	55.82	55.24	55.38	55.61	55.56	55.65	52.56	52.47	54.56
TiO_2	0.53	0.67	0.62	0.45	0.45	0.43	0.44	0.43	–	0.47
FeO	13.89	13.72	13.91	13.50	13.29	13.10	13.11	14.10	14.76	13.90
MnO	0.16	0.16	0.14	0.24	0.17	0.18	0.18	0.03	0.09	0.04
MgO	1.15	1.17	1.17	0.92	0.85	0.87	0.89	1.66	1.69	1.81
CaO	–	–	0.01	0.02	–	–	–	0.07	0.07	0.04
Na_2O	0.01	0.03	0.01	0.05	0.05	0.05	0.05	–	0.07	0.10
K_2O	0.01	–	0.01	–	–	0.01	–	–	0.02	0.01
ZnO	0.16	0.36	0.09	1.85	1.82	1.76	1.55	0.66	0.66	0.67
Total	99.60	98.87	99.62	99.84	99.98	99.93	99.97	97.40	98.12	99.53
46 O										
Si	7.51	7.30	7.61	7.44	7.55	7.67	7.66	7.67	7.76	7.62
Al	17.90	18.14	17.75	18.01	17.96	17.81	17.84	18.02	17.29	17.49
Ti	0.12	0.14	0.13	0.09	0.09	0.09	0.09	0.09	0.10	0.10
Cr	0.02	0.01	0.03	0.03	0.02	0.01	0.01	–	–	0.02
Fe^{+2}	3.34	3.33	3.34	3.06	2.99	2.98	2.97	3.19	3.45	3.39
Mn	0.04	0.04	0.03	0.06	0.04	0.04	0.05	0.01	0.02	0.01
Mg	0.46	0.47	0.47	0.37	0.36	0.39	0.39	0.63	0.70	0.73
Ca	–	–	–	0.01	–	–	–	0.02	0.02	0.01
Na	0.01	0.02	0.01	0.03	0.04	0.03	0.04	–	0.04	0.05
K	–	–	0.01	–	–	–	–	–	0.01	–
Zn	0.03	0.07	0.02	0.37	0.36	0.35	0.31	–	0.14	0.14
$Fe^{+2}/(Fe^{+2} + Mg)$	0.88	0.88	0.88	0.84	0.83	0.82	0.89	0.89	0.88	0.88

aceous schists compose euhedral crystals with sharp boundaries (Fig. 3j).

The late-kinematic garnet generation comprises subhedral grains of this mineral without pressure shadows (Fig. 4a). Garnet grains of this generation can be readily identified by the presence of randomly oriented inclusions, with some of these porphyroblasts containing no inclusions and noted for their low Mn concentrations. Their outlines clearly cut across the schistosity. Postkinematic garnet occurs in the metapelites within the staurolite–andalusite, staurolite–sillimanite, and sillimanite–muscovite metamorphic zones.

The *sheet silicates* of the metapelitic rocks are muscovite, biotite, and chlorite. The early-kinematic generation of these minerals defines the schistosity of the rock matrix and pressure shadows around garnet grains in the garnet–chlorite zone (Fig. 3a). The biotite and muscovite of the late-kinematic generation occur as elongated subhedral laths, which cut the schistosity and fragmentary replace the rims of garnet grains in the staurolite–andalusite, staurolite–sillimanite, and sillimanite–muscovite metamorphic zones (Fig. 4a).

When studying the Tim–Yastrebovskaya structure metapelites, we get conducted more than 400 microprobe spot analyses of garnet, the most representative and typical of which are listed in Table 7.

In accordance with its composition (Mn concentration), the garnet of the garnet–chlorite zone can be subdivided into the following types (Fig. 5):

(a) relatively Fe-rich garnet (Figs. 3a, 3d);

(b) relatively Mn-rich garnet (Figs. 3g).

The garnet of the former type (Samples 3615/1, 2215/9) is characterized by X_{Fe} = 89–94% and contains 13–34% spessartine, 4–9% pyrope, and 5–18% grossular (Table 7). These garnet grains display clear prograde growth zoning in terms of Ca, Mg, Fe, and Mn concen-

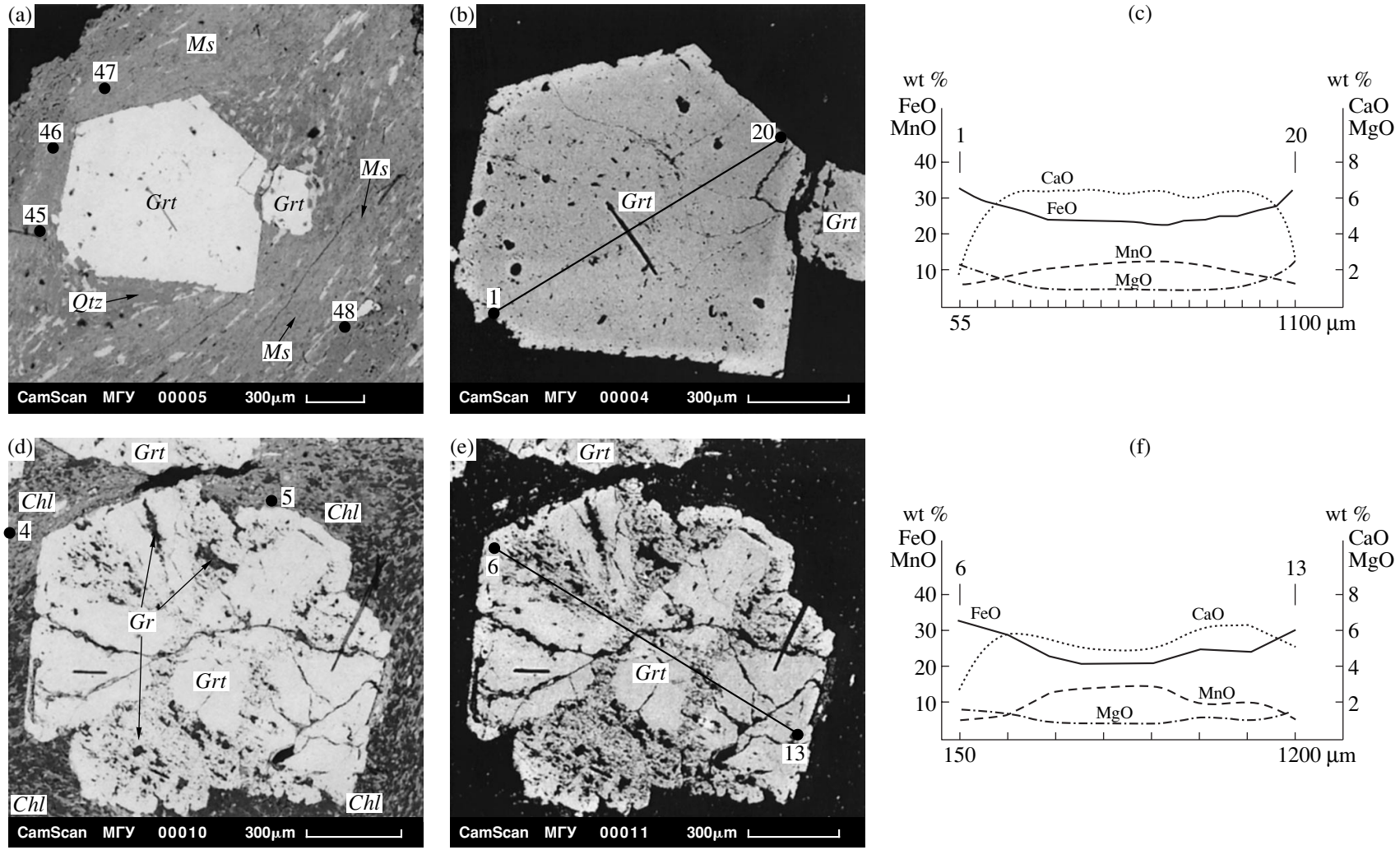

Fig. 3. Morphological types (images in back-scattered electrons) and zoning (microprobe profiles) of garnet from the chlorite zone.
Morphological types of garnet: (a, b, d, e) high-Fe early kinematic; (g, h, j) high-Mn early kinematic.
Microprobe profiles across garnet grains: (c, f) high-Fe early kinematic; (i, k) high-Mn early kinematic.

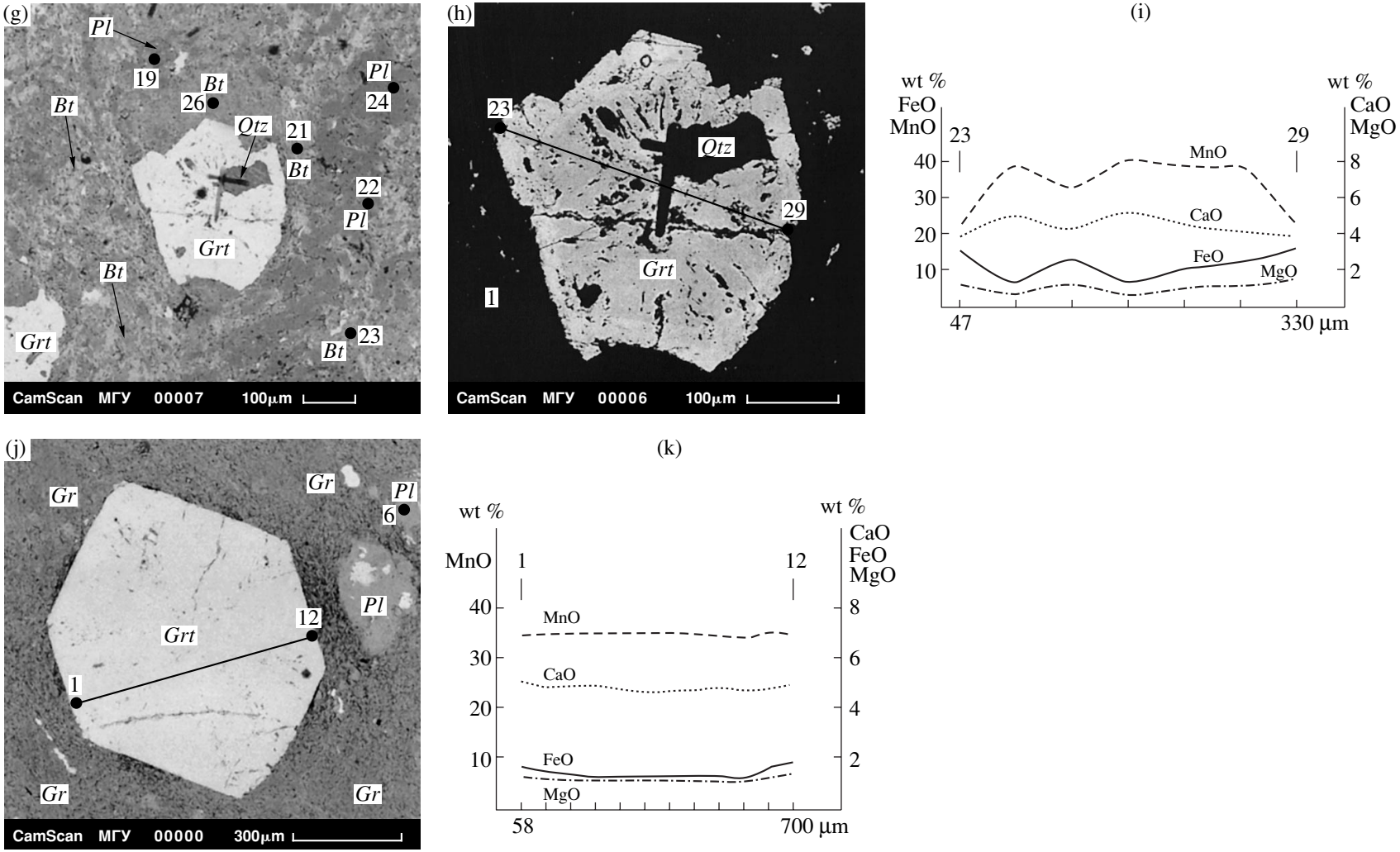
(g)
Pl
19
Bt
26
Bt
Qtz
21
Bt
Pl
24
22
Pl
Grt
Bt
Grt
23
Bt
CamScan МГУ 00007 100μm
(h)
23
Qtz
29
Grt
1
CamScan МГУ 00006 100μm
(i)
wt %
FeO
MnO
wt %
CaO
MgO
23
29
MnO
CaO
FeO
MgO
40
30
20
10
8
6
4
2
47
330 μm
(j)
Gr
Gr
Pl
6
Pl
12
Grt
1
Gr
Gr
CamScan МГУ 00000 300μm
(k)
wt %
wt %
MnO
CaO
FeO
MgO
1
12
MnO
CaO
FeO
MgO
40
30
20
10
8
6
4
2
58
700 μm

Fig. 3. (Contd.)

Table 7. Microprobe analyses of garnet from metapelites of the Tim–Yastrebovskaya structure

Component	Garnet–chlorite zone												Staurolite–andalusite zone			Staurolite–sillimanite zone			Sillimanite–muscovite zone		
	3063/1a			3615/1			3678/256.0			2215/9			3670/1			4317/370.1			3704/20		
	profile with spot analyses spaced 58 μm apart			profile with spot analyses spaced 55 μm apart			profile with spot analyses spaced 47 μm apart			profile with spot analyses spaced 150 μm apart			profile with spot analyses spaced 58 μm apart			profile with spot analyses spaced 250 μm apart			profile		
	margin	core	margin	margin	core	margin	margin	core	margin	margin	core	margin	margin	core	margin	margin	core	margin	margin	core	margin
	Grt-1	*Grt*-7	*Grt*-12	*Grt*-1	*Grt*-9	*Grt*-20	*Grt*-23	*Grt*-26	*Grt*-29	*Grt*-6	*Grt*-9	*Grt*-13	*Grt*-14	*Grt*-17	*Grt*-20	*Grt*-1	*Grt-4*	*Grt*-8	*Grt*-39	*Grt*-41	*Grt*-42
SiO_2	35.74	36.57	36.20	36.20	36.00	35.85	36.38	35.81	36.34	35.94	36.68	36.22	36.04	35.35	36.02	39.47	36.42	35.97	36.53	35.39	35.04
Al_2O_3	20.52	20.32	21.29	20.59	20.44	20.91	22.24	21.02	22.01	22.03	21.74	21.95	21.91	21.42	21.39	21.78	21.70	21.60	21.90	23.19	24.51
TiO_2	0.09	0.53	0.19	0.04	0.14	–	–	0.62	0.06	0.01	0.07	0.07	0.01	0.07	–	0.07	0.07	0.09	0.04	1.37	0.09
Cr_2O_3	–	–	–	–	–	–	–	–	–	–	–	–	–	–	–	0.04	–	0.12	–	–	–
FeO	1.98	1.46	1.82	32.82	23.88	32.57	15.51	6.32	15.32	32.89	21.05	30.19	34.34	33.92	34.93	37.07	36.22	37.43	35.19	34.57	35.11
MnO	33.72	34.60	34.05	5.96	11.51	6.31	19.15	25.02	19.20	5.42	14.44	5.58	3.59	2.80	3.51	0.45	0.43	0.32	0.29	0.24	0.27
MgO	1.45	1.25	1.38	2.39	0.90	2.34	1.28	0.63	1.55	1.65	0.94	1.53	1.84	2.45	1.88	2.42	2.38	2.01	2.88	2.62	2.47
CaO	4.59	4.76	4.86	1.79	6.54	1.94	4.43	7.83	4.53	2.68	4.96	5.03	1.82	2.03	1.40	2.80	2.74	2.71	1.11	1.07	1.69
Total	98.09	99.55	99.80	99.72	99.41	99.92	98.99	97.25	99.01	100.6	99.88	100.6	99.54	98.04	99.11	101.1	99.95	100.3	97.94	98.45	99.18
12 O																					
Si	2.96	2.98	2.95	2.96	2.98	2.93	2.99	2.95	2.99	2.91	2.97	2.92	2.96	2.96	2.95	3.04	2.94	2.92	2.91	2.82	2.80
Al	2.04	1.95	1.51	1.98	1.96	2.01	2.10	2.04	2.08	2.10	2.07	2.08	2.09	2.06	2.07	1.98	2.07	2.07	2.25	2.32	2.39
Ti	0.01	0.03	0.03	–	0.01	–	–	0.04	–	–	–	–	–	–	–	–	–	0.01	–	0.08	0.01
Cr	–	–	–	–	–	–	–	–	–	–	–	–	–	–	–	–	–	0.01	–	–	–
Fe^{+2}	0.13	0.10	0.14	2.24	1.62	2.22	1.04	0.44	1.03	2.23	1.42	2.03	2.32	2.31	2.40	2.39	2.45	2.54	2.34	2.30	2.35
Mn	2.30	2.39	2.32	0.41	0.79	0.44	1.30	1.75	1.30	0.37	0.99	0.38	0.25	0.19	0.24	0.03	0.03	0.02	0.02	0.02	0.02
Mg	0.17	0.15	0.16	0.29	0.12	0.29	0.15	0.08	0.19	0.20	0.11	0.18	0.22	0.30	0.23	0.28	0.29	0.24	0.34	0.31	0.29
Ca	0.4	0.42	0.42	0.16	0.57	0.17	0.38	0.69	0.39	0.23	0.43	0.43	0.16	0.18	0.12	0.23	0.24	0.24	0.10	0.09	0.15
$Fe^{+2}/(Fe^{+2} + Mg)$	0.43	0.41	0.47	0.89	0.94	0.89	0.87	0.85	0.85	0.92	0.93	0.92	0.91	0.89	0.91	0.90	0.90	0.91	0.87	0.88	0.89
Alm	0.04	0.03	0.05	0.72	0.53	0.71	0.36	0.15	0.35	0.74	0.48	0.67	0.79	0.78	0.80	0.82	0.82	0.84	0.84	0.85	0.84
Sps	0.77	0.78	0.76	0.13	0.25	0.14	0.45	0.59	0.45	0.12	0.34	0.13	0.08	0.07	0.08	0.01	0.01	0.01	0.01	0.01	0.01
Prp	0.06	0.05	0.05	0.09	0.04	0.09	0.05	0.03	0.06	0.07	0.04	0.06	0.08	0.10	0.08	0.10	0.10	0.08	0.12	0.11	0.12
Grs	0.13	0.14	0.14	0.05	0.18	0.05	0.13	0.23	0.13	0.08	0.15	0.14	0.05	0.06	0.04	0.08	0.08	0.08	0.03	0.03	0.05

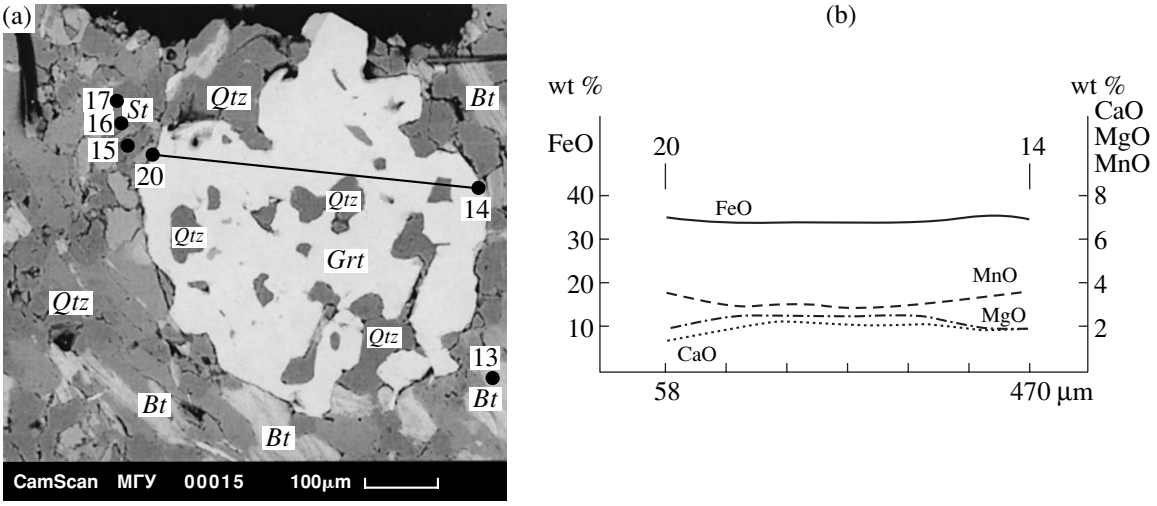

Fig. 4. Late-kinematic garnet from the staurolite–andalusite zone.
(a) Back-scattered electron image. (b) Microprobe profile.

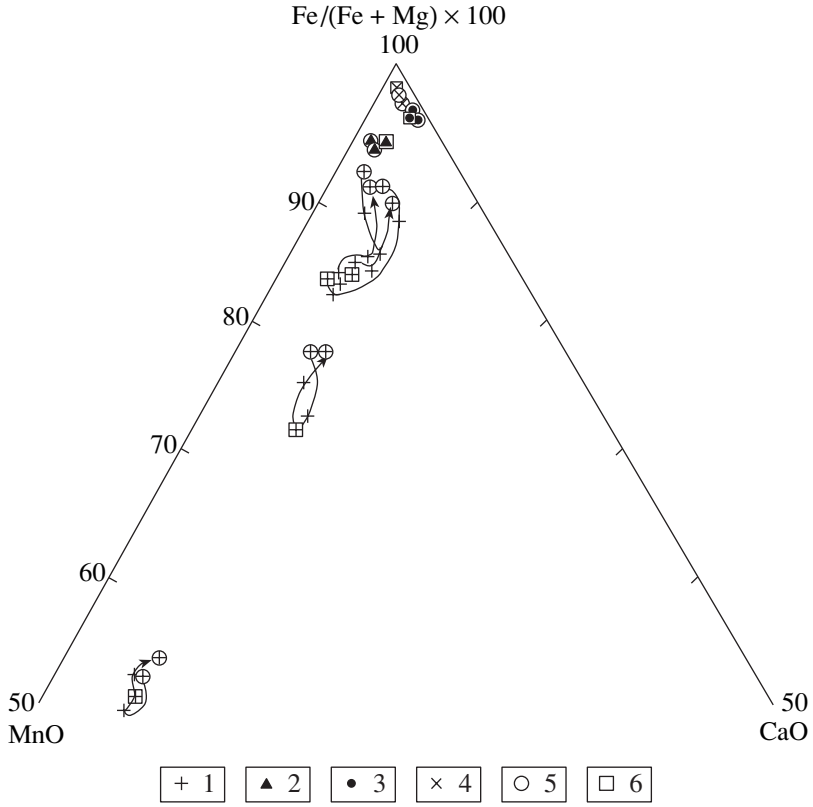

Fig. 5. Composition of garnet from metapelites of different metamorphic zones of the Tim–Yastrebovskaya structure.
(1–4) Garnet composition: (1) garnet from the garnet–chlorite zone, (2) garnet from the staurolite–andalusite zone, (3) garnet from the staurolite–sillimanite zone, (4) garnet from the sillimanite–muscovite zone; (5) margin of a garnet grain; and (6) core of a garnet grain.

trations. The CaO and MnO concentrations decrease, whereas those of FeO and MgO increase from the cores of rims of crystals (Figs. 3c, 3f).

The garnet of the second type (Sample 3678/256.0) has X_{Fe} = 85–87% and is notably enriched in MnO (19–25 wt %). The concentrations of the spessartine, grossular, and pyrope and-members are, respectively, 45–59, 13–23, and 3–6% (Table 7). The clear zoning is also prograde (Fig. 3i). The elevated MnO concentrations of most of the garnets is explained by the fact that, in the

absence of other Mn-bearing minerals, garnet is the only phase of the garnet–chlorite zone capable of concentrating this component.

Garnet from the carbonaceous sulfide-bearing schists compose an individual field (Fig. 5). The garnet is spessartine with a low concentration (13–16%) of grossular (Table 7), which is explained by the bulk-rock chemistry of the carbonaceous schists. The poorly pronounced zoning of this mineral is discernible only in the distribution of Fe and Mg, whose concentrations increase from cores to rims (Fig. 3k).

The high-Mn and low-Mn rocks of the staurolite–andalusite and staurolite–sillimanite metamorphic zones contain Fe-richer garnet, whose content strongly increases in Mn-rich rocks.

The iron mole fraction of garnet in the staurolite–andalusite zone equals 89–91%. This garnet is poorer in spessartine (7–8%) and grossular (5–7%) (Table 7) and differs from this mineral in the garnet–chlorite zone by lower concentrations of MnO (2.8–3.5 wt %, Table 7). The MnO concentration increases and MgO simultaneously decreases from the cores to rims of crystals, i.e., the garnet zoning is retrograde (Fig. 4b).

Garnet in the assemblages of the staurolite–sillimanite zone is characterized by X_{Fe} = 90–91%, with the MnO concentration decreasing to 0.32–0.45 wt % (Table 7). No clear zoning was detected (Fig. 6).

Garnet occurs in the metapelites of the sillimanite–muscovite zone as dodecahedral grains devoid of inclusions. The X_{Fe} ranges from 87 to 89%, and the concentrations of the spessartine, grossular, and pyrope components are, respectively, 1, 3–5, and 11–12% (Table 7). Compared with the garnet of the staurolite–sillimanite zone, the garnet of this zone is slightly lower in Mn and higher in Fe. The garnet of Sample 3704/20 displays retrograde zoning (the FeO and MnO concentrations increase rimward). The increase in the X_{Mg} of garnet toward its contact with biotite is explained by the exchange reaction $Bt_{Mg} + Grt_{Fe} \longrightarrow Bt_{Fe} + Grt_{Mg}$.

METAMORPHIC REACTIONS

The appearance and growth of garnet in the garnet–chlorite zone of the Tim–Yastrebovskaya structure proceed by means of reaction between chlorite and quartz

$$Chl_{<Fe} + Qtz \longrightarrow Chl_{Fe<} + Grt_{Fe} + H_2O. \quad (1)$$

This reaction leads to an increase in the X_{Fe} of garnet and a decrease in this parameter of chlorite.

The appearance and growth of staurolite in relatively Fe- and Al-rich metapelites is associated with the decomposition of chlorite *per se* or its assemblages with garnet

$$Chl + Ms \longrightarrow St + Bt + Qtz + H_2O \quad (2)$$

$$Ms + Grt + Chl \longrightarrow St + Bt + Qtz + H_2O. \quad (3)$$

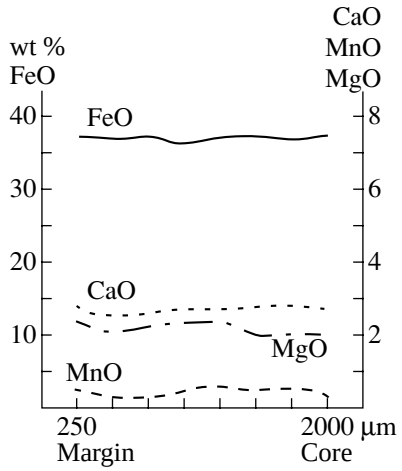

Fig. 6. Microprobe profile across a garnet grain from the staurolite–sillimanite zone.

However, staurolite does not appear at all in Mn-enriched rocks because of the stability of the right-hand side of the hypothetical reaction

$$St + MnO + Ms \pm Qtz \longrightarrow Bt + Grt_{Mn-Fe(Ca, Mg)} + And. \quad (4)$$

Sillimanite is produced in the higher grade parts of the staurolite–sillimanite zone by both the $And \longrightarrow Sil$ inversion and the partial decomposition of staurolite

$$St + Qtz + Ms \longrightarrow Bt + Sil + Grt + H_2O \quad (5)$$

and the possible prograde breakdown of the Na-richest muscovite

$$Ms_{Na} + Qtz \longrightarrow Ms_{Na<} + Ab(Olg) + Sil + H_2O. \quad (6)$$

An increase in the temperature results in the resorption of staurolite, decrease in its X_{Fe}, and an increase in the ZnO concentration in the last remaining staurolite by the reaction

$$St + Qtz \longrightarrow Grt + Sil + St_{>Zn} + H_2O. \quad (7)$$

The carbonaceous schists provide evidence of two reactions

$$Grt_{Fe-Mn} + S_2 \longrightarrow Pyr + Grt_{Mn} \quad (8)$$

$$Bt_{Fe-Mg} + S_2 \longrightarrow Bt_{Mg} + Pyr. \quad (9)$$

P–T METAMORPHIC CONDITIONS

The *P–T* metamorphic conditions of the Tim–Yastrebovskaya metapelites were determined by two methods. First, we compared the mineral assemblages observed in the rocks with known petrogenetic grids (Korikovskii, 1979 and others) and the experimentally established boundaries of the stability fields of minerals and mineral assemblages (for example, aluminosilicates, staurolite with quartz, and others). The advantage

Table 8. Metamorphic temperatures calculated for metapelites of the Tim–Yastrebovskaya structure

Sample	Thermometer	Temperature, °C
	Garnet–chlorite zone	
3678/256.0	*Grt*(margin) – *Bt*(21) (Perchuk, 1986)	501
	Grt(margin) – *Bt*(21) (Ferry, Spear, 1978)	410
	Grt(margin) – *Bt*(21) (Thompson, 1976)	450
2215/2	*Grt*(13) – *Chl*(matrix) (Perchuk, 1989)	465
	Grt(13) – *Chl*(matrix) (Patric, Evans, 1989)	463
3615/1	*Grt*(margin) – *Ms*(45) (Hanes, Forest, 1988)	420
	Grt(margin) – *Ms*(45) (Krogh, Raheim, 1978)	502
	Staurolite–andalusite zone	
3670/1	*Grt*(20) – *Bt*(matrix) (Perchuk, 1986)	506
	Grt(20) – *Bt*(matrix) (Ferry, Spear, 1978)	503
	Grt(20) – *Bt*(matrix) (Thompson, 1976)	519
	Staurolite–sillimanite zone	
4317/370.1	*Grt*(margin) – *Bt*(incl. in *Grt*) (Perchuk, 1986)	534
	Grt(margin) – *Bt*(incl. in *Grt*) (Ferry, Spear, 1978)	510
	Grt(margin) – *Bt*(incl. in *Grt*) (Thompson, 1976)	524
3716/1	*Ms*(matrix) – *Bt*(matrix) (Hoisch, 1989)	531
	Sillimanite–muscovite zone	
3704/20	*Grt*(margin) – *Bt*(matrix) (Perchuk, 1986)	601
	Grt(margin) – *Bt*(matrix) (Ferry, Spear, 1978)	617
	Grt(margin) – *Bt*(matrix) (Thompson, 1976)	617
	Grt(margin) – *St*(incl. in *Grt*) (Perchuk, 1989)	583

of this method is its capability of determining the overall position of the assemblages in a *P–T* space and the character of metamorphism (facies series). This technique can be particularly successfully applied to medium-temperature metapelites, in which a relatively narrow temperature interval may involve the appearance and decomposition of several minerals (for example, chlorite, staurolite, muscovite, etc.), which systematically vary in composition. At the same time, this technique is disadvantageous because it often cannot provide precise quantitative *P–T* estimates.

The second method, mineralogical thermobarometry, makes use of the composition of chemically zoned minerals to reconstruct *P–T* coordinates and paths. These techniques can be more successfully utilized in calculating the *P–T* trajectories of high-temperature rocks, because the careful interpretation of thermobarometric results potentially offers valuable information on the evolution of the metamorphic complexes. The disadvantage of this method is the possibility of errors caused by the poorly known thermodynamic constant of some mineral solid solutions and the affect of some components (such as MnO in garnet or ZnO in staurolite) on the properties of the minerals, as well as by difficulties in determining the equilibrium compositions of minerals utilized in thermobarometry.

In order to assay the temperatures of the earlier metamorphic episode we used the compositions of the early-kinematic garnet and the garnet–biotite (Perchuk, 1986; Thompson, 1976; Ferry and Spear, 1978), garnet–chlorite (Perchuk, 1989; Patric and Evans, 1989), and garnet–muscovite (Hanes and Forest, 1988; Krogh and Raheim, 1978) thermometers (Table 8). We utilized the compositions of the marginal parts of garnet grains with prograde zoning and the compositions of adjacent biotite, muscovite, and chlorite in the rock matrix.

The pressure was quantified by the garnet–plagioclase–andalusite–quartz geobarometer (Aranovich and Podlesskii, 1980; Table 9) with the use of the compositions of garnet in the margins of grains with prograde zoning and the matrix plagioclase.

Our results indicate that the Tim–Yastrebovskaya metapelites underwent metamorphism to the garnet–chlorite grade during the early stage. The metamorphic conditions corresponded to the high-grade greenschist facies with temperatures of 420–500°C and pressures of 3.0–3.1 kbar.

The thermodynamic parameters of the higher temperature metamorphic episode were quantified based on the compositions of late-kinematic garnet and the garnet–biotite (Perchuk, 1986; Thompson, 1976; Ferry and Spear, 1978), garnet–staurolite (Perchuk, 1989),

Table 9. Metamorphic pressures calculated for metapelites of the Tim–Yastrebovskaya structure

Sample	Barometer	*P*, kbar
3678/256.0	*Grt*(margin) – *Pl*(22) (Aranovich and Podlesskii, 1980)	3.1
	Grt(core) – *Pl*(19) (Aranovich and Podlesskii, 1980)	3.0

Note: Numbers in parentheses correspond to the numbers of microprobe spot analyses in Figs. 3 and 4.

and biotite–muscovite (Hoisch, 1989) geothermometers. The compositions of the minerals were measured in the margins of garnet crystals with retrograde zoning and adjacent matrix biotite (Samples 3670/1 and 3704/20), margins of unzoned garnet grains and biotite inclusions in them (Sample 4371/370.1), margins of garnet grains with retrograde zoning and staurolite inclusions in this garnet (Sample 3704/20), and matrix muscovite and adjacent matrix biotite (Sample 3716/1). We have determined that the metapelites were metamorphosed to the staurolite-andalusite subfacies at 500–520°C, staurolite–sillimanite subfacies at 520–580°C, and sillimanite–muscovite subfacies at 580–620°C (Table 8).

We failed to evaluate the pressure with the use of known geobarometers because of the rarity of suitable mineral assemblages. Because of this, our pressure estimates for the staurolite–andalusite, staurolite–sillimanite, and sillimanite–muscovite zones were based on the results of paragenetic analysis. The presence of the staurolite plus sillimanite assemblage in the metapelites suggests pressures of 3–5 kbar (Korikovskii, 1979), and the occurrence of andalusite in the staurolite–sillimanite zone constrains this interval to 3–4 kbar. The high iron mole fraction of garnet from the sillimanite–muscovite zone also points to pressures of 3–4 kbar (Fig. 7).

THE ORIGIN OF THE TIM–YASTREBOVSKAYA STRUCTURE AND THE METAMORPHIC EVOLUTION OF METAPELITES

In the general geodynamic evolutionary model for the Voronezh crystalline massif, the Tim–Yastrebovskaya structure is currently regarded as a second-order rift-related structure within the Proterozoic continent of the Kursk Magnetic Anomaly (Chernyshov *et al.*, 1997).

Early during Proterozoic time and the most active uplift of the Kursk and Voronezh–Samara continent, the Kursk Magnetic Anomaly was a dry land. An inner continental sea basin existed at the site of the structure in the earliest Proterozoic. In lagoons of this basin, terrigenous sediments and the clayey redeposition products of weathering crusts were accumulated. This time period was also responsible for the deposition of chemogenic carbonate–iron formations (the Kursk Group and the Rogovskaya Formation of the Oskol'skaya Group). Changes in the steady-state thermal regime brought about the reactivation of the Kursk block and the onset of a prerift stage, when an extensive uplift started to develop in place of the shallow-water basin. Its growth was coupled with active volcanism and conglomerate deposition on the slopes. A still-shallow northwest-trending rift trough started to develop during the early rifting stage in the axial, weakened zone of the uplift. As the trough evolved, the subsidence became progressively more intense, and thick masses of fine-grained and graywacke silty metapelites began to fill the structure. The sedimentation process was accompanied by active volcanism, which extended outside the Tim–Yastrebovskaya structure. Sedimentation and volcanism of the late rifting stage were concentrated only within the progressively deepening trough. The closing rifting stages of the structure were marked by the transition from fine terrigenous and chemogenic sediments to continental molasses. The closure of the Tim–Yastrebovskaya rift was induced by collision between the Kursk and Voronezh–Samara geoblocks. The onset of compression, which was oriented from northeast to southwest, caused extensive imbrication and overthrusting within the structure. The growth of a folded orogen at the site of the rift trough was accompanied by the first episode of regional metamorphism.

The U–Pb age of volcanism that produced the Timskaya Formation of the Oskol'skaya Group is 2254 Ma (it was determined on zircon from acid volcanics that rest conformably with the rock of the formation; Artemenko *et al.*, 1992). It can be hypothesized that

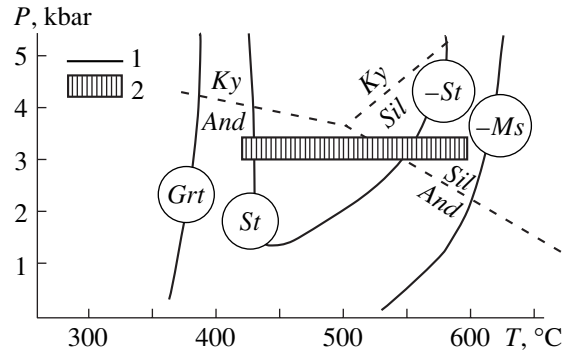

Fig. 7. *P–T* metamorphic parameters of metapelites in the Tim–Yastrebovskaya structure.

(1) Boundaries of metamorphic facies (given after Korikovskii, 1979) and isograds of the appearance and disappearance of minerals (for example, (St) and (–St) correspond to staurolite-in and staurolite-out isograds, respectively); (2) *P–T* region of metamorphism of metapelites from the Tim–Yastrebovskaya structure.

regional metamorphism of the Tim–Yastrebovskaya deposits proceeded slightly later than 2250 Ma but earlier than the intrusion of the postmetamorphic granodiorites of the Stoilo–Nikolaevskii Complex, which was dated at 2086 Ma (Artemenko *et al.*, 1992).

The compressional environment predetermined the appearance of a number of crustal melting zones, which caused the intrusion of granodiorites of the Stoilo–Nikolaevskii Complex after the closure of the Tim–Yastrebovskaya rift. The igneous rocks served as the sources of heat for younger contact–regional metamorphism, which occurred locally and produced the staurolite–andalusite, staurolite–sillimanite, and sillimanite–muscovite metamorphic zones.

Intrusions of this complex were dated at 2086 ± 5 Ma (Artemenko *et al.*, 1992). The metamorphic event that produced the metamorphics, including the metapelites, should have been coeval with these magmatic processes.

Hence, a young platform area appeared in the Tim–Yastrebovskaya rift structure late in the Early Proterozoic.

CONCLUSION

1. The rarity of staurolite in the mineral assemblages of the Tim–Yastrebovskaya structure is explained by the wide occurrence of metapelites originally enriched in Mn. Instead of staurolite, these rocks contain the stable assemblage of Mn-rich garnet and andalusite.

2. The garnet of the rocks can be subdivided into two generations: early kinematic with respect to the D1 stage and related to the folding and late kinematic which occurs near intrusive bodies.

3. The study of the Tim–Yastrebovskaya metapelites has demonstrated that the metamorphic zoning within the structure was determined by the heat flow from intruded magmatic bodies. The following metamorphic zones were distinguished: garnet–chlorite, staurolite–andalusite, staurolite–sillimanite, and sillimanite–muscovite. The garnet–chlorite zone was related to regional metamorphism; the staurolite–andalusite, staurolite–sillimanite, and sillimanite–muscovite zones developed locally and are spatially restricted to compositionally variable intrusive bodies.

4. The Tim–Yastrebovskaya metapelites underwent prograde metamorphism at T = 420–500°C, P_{tot} = 3.0–3.1 kbar in the garnet–chlorite zone; T = 500–520°C in the staurolite–andalusite zone; T = 520–580°C in the staurolite–sillimanite zone; and T = 580–620°C at P_{tot} = 3–4 kbar in the sillimanite–muscovite zone.

5. The Tim–Yastrebovskaya structure was affected by two metamorphic episodes: early regional metamorphism to the garnet–chlorite grade at 2250–2086 Ma and younger high-temperature contact metamorphism at 2086 ± 5 Ma. The latter event produced the metamorphic zoning observable within the structure.

ACKNOWLEDGMENTS

This study was supported by the Integration Federal Program (project C0007), Universities of Russia Program (project 990087), a grant from the President of the Russian Federation (project 00-15-99397), and the Russian Foundation for Basic Research (project nos. 00-05-64522, 01-05-06203).

REFERENCES

Aranovich, L.Ya. and Podlesskii, K.V., Garnet–Plagioclase Geobarometer, *Dokl. Akad. Nauk SSSR*, 1980, vol. 251, no. 5, pp. 1216–1219.

Artemenko, G.V., Bartnitskii, E.N., and Myasnyankin, V.I., The U–Pb Age of Igneous Rocks from Orlovsko–Timskii Greenstone Structure of the Voronezh Crystalline Massif, *Dokl. Akad. Nauk Ukr.*, 1992, no. 7, pp. 113–117.

Chernyshov, N.M., Nenakhov, V.M., Lebedev, I.P., *et al.*, A Model for the Geodynamic Development of the Voronwezh Crystalline Massif, *Geotektonika*, 1997, no. 3, pp. 21–30.

De Yoreo, J.J., Lux, D.R., and Guidotti, C.V., Thermal Modeling in Low Pressure/High Temperature Metamorphic Belts, *Tectonophysics*, 1991, vol. 188, pp. 253–268.

Dobretsov, N.L., Reverdatto, V.V., Sobolev, V.S., *et al.*, *Fatsii metamorfizma* (Facies of Metamorphism), Moscow: Nedra, 1970, vol. 1.

England, P.C. and Thompson, A.B., Pressure–Temperature–Time Paths of Regional Metamorphism: I. Heat Transfer during the Evolution of Regions of Thickened Continental Crust, *J. Petrol.*, 1984, vol. 25, part 4, pp. 894–928.

Ferry, J.M. and Spear, F.S., Experimental Calibration of the Partitioning of Fe and Mg between Biotite and Garnet, *Contrib. Mineral. Petrol.*, 1978, vol. 66, pp. 113–117.

Fonarev, V.I., Graphchikov, A.A., and Konilov, A.N., A Consistent System of Geothermometers for Metamorphic Complexes, *Int. Geol. Rev.*, 1991, vol. 33, no. 8, pp. 743–783.

Gerya, T.V. and Perchuk, L.L., GEOPATH: A New Computer for Geothermobarometry and Related Calculations with the IBM PC Computer, *Int. Miner. Assoc. The 15th General Meeting*, Abstracts of Papers, Beijing, 1992, vol. 2, p. 1010.

Glebovitskii, V.A., Geological and Physicochemical Relation between Metamorphism and Tectonics in Early Precambrian, *Geotektonika*, 1996, no. 5, pp. 27–42.

Hanes, A. and Forest, R.C., Empirical Garnet–Muscovite Geothermometry in Low-Grade Metapelites, Selwyn Range (Canadian Rockies), *J. Metamorph. Geol.*, 1988, vol. 6, no. 6, pp. 297–309.

Hoisch, T.D., A Muscovite–Biotite Geothermometer, *Am. Miner.*, 1989, vol. 74, no. 5/6, pp. 565–572.

Korikovskii, S.P., Contrasting Models of the Metamorphic Prograde–Retrograde Evolution of Phanerozoic Fold Belts in Collision and Subduction Zones, *Petrologiya*, 1995, vol. 3, no. 1, pp. 45–63.

Korikovskii, S.P., *Fatsii metamorfizma metapelitov* (Metamorphic Facies of Metapelites), Moscow: Nauka, 1979.

Krogh, E.J. and Raheim, A., Temperature and Pressure Dependence of Fe–Mg Partitioning between Garnet and Phengite, with Particular Reference to Eclogite, *Contrib. Mineral. Petrol.*, 1978, vol. 66, pp. 75–80.

Patric, B.E. and Evans, B.W., Metamorphic Evolution of the Seaward Peninsula Blueschist Terrane, *J. Petrol.*, 1989, vol. 30, no. 3, pp. 351–555.

Perchuk, L.L., Evolution of Metamorphism, in *Eksperiment v reshenii aktual'nykh zadach geologii* (Experiment in Solving Topical Problems of Geology), Moscow: 1986, pp. 151–173.

Perchuk, L.L., Mutual Coordination of Some Fe–Mg Geothermometers on the Basis of the Nernst Law: A Revision, *Geokhimiya*, 1989, no. 5, pp. 611–622.

Reverdatto, V.V., Sheplev, V.S., and Polyanskii, O.P., Burial Metamorphism and the Evolution of Rift Basins: A Simulating Approximation, *Petrologiya*, 1995, vol. 3, no. 1, pp. 37–44.

Savko, K.A., Sillimanite–Muscovite Zone in the Metamorphic Complex of the Vorontsovskaya Group of the Voronezh Crystalline Massif, *Geol. Geofiz.*, 1994, no. 6, pp. 73–86.

Thompson, A.B., Mineral Reactions in Pelitic Rocks: 2. Calculation of Some *P–T–X* (Fe–Mg) Phase Relations, *Am. J. Sci.*, 1976, no. 4, pp. 425–454.